

# Numerical Analysis of Flow past Circular Cylinder with Triangular and Rectangular Wake Splitter

Pavan Badami, Vivek Shrivastava, Saravanan V., Nandeesh Hiremath, K. N. Seetharamu

**Abstract**—In the present work flow past circular cylinder and cylinder with rectangular and triangular wake splitter is studied to improve aerodynamic parameters. The Comparison of drag coefficient is tabulated for bare cylinder, cylinder with rectangular and triangular wake splitters. Flow past circular cylinder and cylinder with triangular and rectangular wake splitter is performed at Reynolds number 5, 20, 40, 50, 80, 100. An incompressible PISO finite volume code employing a non-staggered grid arrangement is used, a second order upwind scheme is used for convective terms. The time discretization is implicit and a Second order Crank-Nicholson scheme is employed. Length of wake splitter in both configurations is taken to be equal to diameter of cylinder. Wake length is found to be less with rectangular wake splitter when compared to bare cylinder and cylinder with triangular wake splitter. Coefficient of drag is found to be less for triangular wake splitter when compared to bare cylinder & cylinder with rectangular wake splitter.

**Keywords**—Coefficient of drag and pressure, CFD-FLUENT, Triangular and rectangular wake splitter, wake length.

## I. INTRODUCTION

PRESENT study considers numerical investigation for incompressible flow over cylinder of diameter  $D$  with and without wake splitter. Flow over a cylinder is a fundamental fluid mechanics problem of practical importance having wide range of applications. Flow over the cylinder is symmetric at low values of Reynolds number. However, as the Reynolds number increases, flow begins to separate behind the cylinder causing symmetric wake formation at Reynolds number less than 50 and vortex shedding (von-Karman vortices) at higher Reynolds number, which is an unsteady phenomenon. Wakes are region of recirculation which is formed behind bluff body. These vortices can cause fluctuations as well as increase in drag forces and can result in serious damage.

Flow around non-streamlined (bluff) body is a challenging kaleidoscopic flow phenomenon. Cylinders of circular, square, or any arbitrary blunt cross-section are examples of two-dimensional bluff bodies. Cross flow normal to the axis of cylinder, square and the associated problems of heat and mass transport are encountered in a wide variety of Industrial and engineering applications.

Pavan Badami, UG Student, Dept. of Mechanical Engineering, PES Institute of Technology, Bangalore, India (pavanbadami@gmail.com)

Vivek Shrivastava, UG Student, Dept. of Mechanical Engineering, PES Institute of Technology, Bangalore, India (wolverine.2392@gmail.com)

Saravanan V, Assistant Professor, Dept. of Mechanical Engineering, PES Institute of Technology, Bangalore, India

Nandeesh Hiremath, UG Student, Dept. of Mechanical Engineering, PES Institute of Technology, Bangalore, India (Hiremath.nandeesh@gmail.com)

K N Seetharamu, Professor, Dept. of Mechanical Engineering, PES Institute of Technology, Bangalore, India

Wind flow around tall chimneys or cooling towers, flow past offshore structures, cross flow around rod bundles in heat exchangers of nuclear reactors, flow past flame stabilizers in high speed combustion chambers flow metering devices, cooling of electronic equipment Pipelines, suspension bridges, poles, cables, Pylons are some of the interesting application examples. Both experimental measurements and numerical computations have confirmed the onset of instability of the wake flow behind a bluff body beyond a critical Reynolds number, leading finally to a kind of periodic flow identified by definite frequencies, well known in the literature as the Von Karman vortex street. This alternate vortex shedding yields a periodic load on the structure and in order to avoid the wind induced large amplitude of oscillation of the structure designer need to know the magnitude and direction of forces in the form drag and lift coefficient.

Splitter plates have been termed as wake stabilizers which are introduced in the downstream of the cylinder. Wake splitters are passive means for controlling various aspects of wake formation and vortex shedding. With the use of splitter plate, pressure drop characteristics can be altered and drag on cylinder can be reduced by making the flow to reattach in the downstream thereby making it streamlined. Various configuration of wake splitter can be used to control vortices.

Work has been carried out on bare cylinder [2], [3], [5] simulated using immersed boundary condition and calculation of force was done using Navier Stokes equation. However present study we have compare the coefficient of Drag with triangular and rectangular splitter plates. Reference [1] carried out simulation with integral wake splitter involving heat transfer. In Present study we have compared aerodynamics of bare cylinder and cylinder with triangular and rectangular wake splitter.

TABLE I  
NOMENCLATURE

SYMBOL	NOMENCLATURE
$D$	Diameter of the cylinder
$\rho$	Density
$X$	Length of the domain
$\mu$	Viscosity
$Y$	Width of the domain
$L$	Length of wake splitter
$Re$	Reynolds number
$L_w$	Length of wake
$C_p$	Coefficient of pressure
$C_D$	Mean coefficient of drag

## II. GRID GENERATION AND BOUNDARY CONDITION

The computation domain for the present work is shown in Fig 1. Computations were performed for circular cylinder of diameter  $D$ . length of flow domain is  $X = 42.5D$  and width  $Y = 25D$ .

For the case of cylinder with rectangular wake splitter, length of wake splitter was taken to be equal to diameter ( $L=D$ ). In this study the following boundary conditions were used. For the flow over a circular cylinder the inlet is placed at a distance of  $12.5D$  upstream of the cylinder where  $U=1, V=0$ . At the outlet the  $u$  velocity is calculated from global continuity together with a zero gradient boundary conditions for both  $U$  and  $V$ . No slip conditions are prescribed at the body surfaces ( $U=V=0$ ). At the upper and lower boundaries symmetry conditions simulating a frictionless wall are used,  $\frac{\partial U}{\partial Y} = V = 0$ .

For the case of cylinder with triangular wake splitter, length of wake splitter was taken to be equal to diameter with splitter having included angle of  $20^\circ$ . A grid refinement study was done to verify the grid independence and the accuracy of the method.

Fig.2 shows uniform mesh of  $168 \times 60$  used in simulations of flow past circular cylinder of diameter  $D$ . Fig.3(a) shows the uniform mesh for rectangular and Fig.3(b) tapered arrangement of wake splitter. Simulation was performed at Reynolds number 5, 20, 40, 50, 80, 100. Required Reynolds number is obtained by varying inlet velocity  $U_\infty$ . The fluid properties  $\rho$  and  $\mu$  were considered constants and were the same for all simulations.

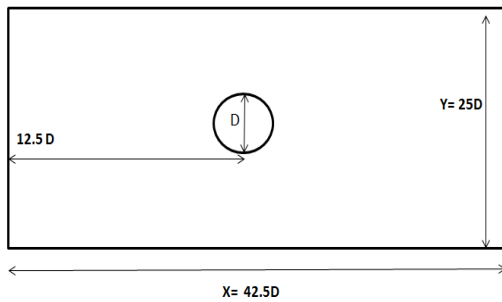


Fig. 1 Computational domain of simulation

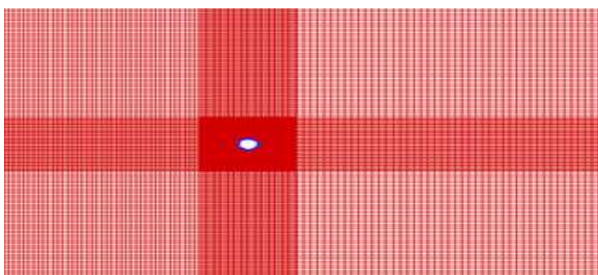


Fig. 2 Uniform mesh generated for cylinder without wake splitter

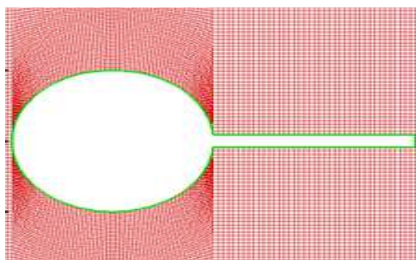


Fig. 3a Mesh generated for rectangular splitter

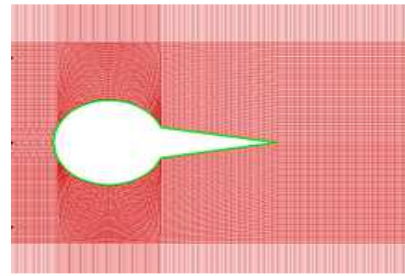


Fig. 3b Mesh generated for triangular splitter

### III. GOVERNING EQUATIONS

Two dimensional continuity, Navier stokes & momentum equations for laminar flow of an incompressible fluid having uniform density

Continuity equation

$$\bullet \quad \frac{\partial u}{\partial x} + \frac{\partial v}{\partial y} = 0 \quad (1)$$

Momentum equation

X momentum equation :

$$\bullet \quad \frac{\partial u}{\partial t} + u \frac{\partial u}{\partial x} + v \frac{\partial u}{\partial y} = -\frac{\partial p}{\partial x} + \frac{1}{\text{Re}} \left[ \frac{\partial^2 u}{\partial x^2} + \frac{\partial^2 u}{\partial y^2} \right] \quad (2)$$

Y momentum equation

$$\bullet \quad \frac{\partial v}{\partial t} + u \frac{\partial v}{\partial x} + v \frac{\partial v}{\partial y} = -\frac{\partial p}{\partial y} + \frac{1}{\text{Re}} \left[ \frac{\partial^2 v}{\partial x^2} + \frac{\partial^2 v}{\partial y^2} \right] \quad (3)$$

### IV. BOUNDARY CONDITIONS

- Top and bottom walls Neumann boundary condition for velocity (due to symmetry) is applied i.e.  $\frac{\partial u}{\partial y} = 0, v = 0$
- Side walls Uniform inlet velocity in  $x$  direction i.e.  $U=1, V=0$  (free slip boundary condition)
- At the cylinder surface No slip condition is applied  $U=0, V=0$

### V. RESULTS AND DISCUSSIONS

#### A. Validation for Single Cylinder

The present simulation of flow past circular cylinder was validated for drag coefficient, with varying Reynolds number 5, 20, 40, 50, 80, 100 with the available numerical results of [2], [3], [5].

TABLE II  
COMPARISON OF MEAN DRAG COEFFICIENT WITH OTHER AUTHORS

Re	Present work	Dennis and chang [2]	Sucker and Brauer [3]	Silva and neto [5]
5	5.92	-	-	-
20	2.254	2.05	2.08	2.04
40	1.706	1.52	1.73	1.54
50	1.55		1.65	1.46
80	1.46		1.51	1.40
100	1.45		1.45	1.39

From the grid independence analysis a  $168 \times 60$  grid was used for the bare cylinder and cylinder with wake splitter arrangement. Computations were carried out for Reynolds number 5, 20, 40, 50, 80, 100 with length of wake splitter as

$L_w=D$ .The residual convergence criterion was satisfied using an upper bound of  $10^{-6}$ .

*B. Effect on streamline contours*

Fig. 4 describes the stream line plots onbare cylinder for Reynolds number equal to 5, 40 and 100. Stream line plots are obtained from commercial software TECPLOT It was observed that at Reynolds number 5 flows is attached in both upstream and downstream of the cylinder. For Reynolds number 5 it is clearly seen that the flow behaves as potential flow, Potential flow is mainly dominated by viscous force and remained attached to the surface. With the increase in Reynolds number flow was found to be attached in upstream but flow got separated on the downstream. Due to phenomena of flow separation recirculating bubble is observed which is defined as wake region .With the increase in Reynolds number, length of the wake region was observed to be increasing behind the cylinder till the attainment of critical Reynolds number 50, which is in agreement with the well-established results, by the linear stability theory. The cylinder wake instabilities rises for  $Re =50$ , as per the simulation performed. Wake was found to be asymmetric for the Reynolds number 50 and above as observed in Fig.4(c).

Similar trend of streamlines is observed for the case of cylinder with rectangular wake splitter as shown in Fig.5 and cylinder with triangular wake splitter in Fig.6.

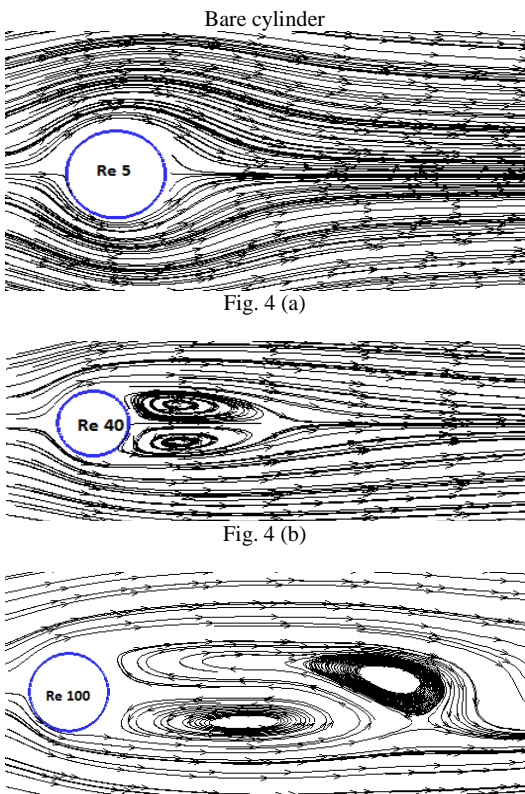


Fig. 4 ( c )

Fig. 4 Stream traces of cylinder without wake splitter  
Rectangular splitter

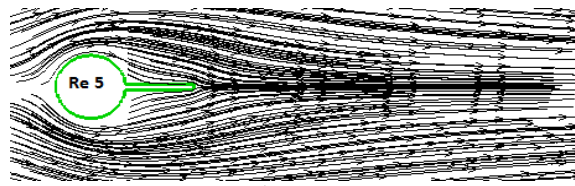


Fig. 5 (a)

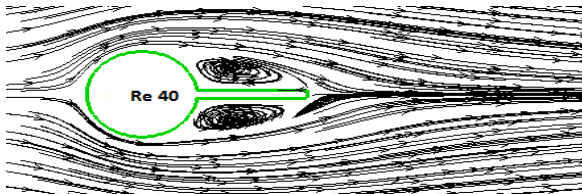


Fig. 5 (b)

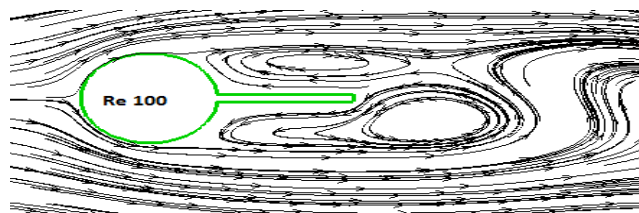


Fig. 5 (c)

Fig. 5 Stream traces of cylinder with rectangular wake splitter

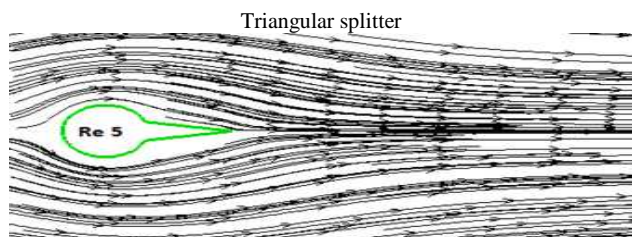


Fig. 6 (a)

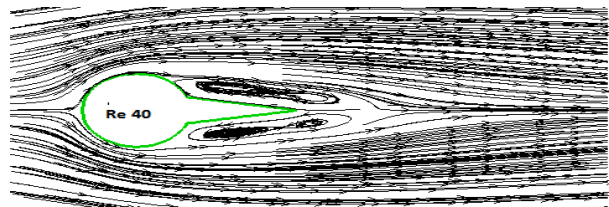


Fig. 6 (b)

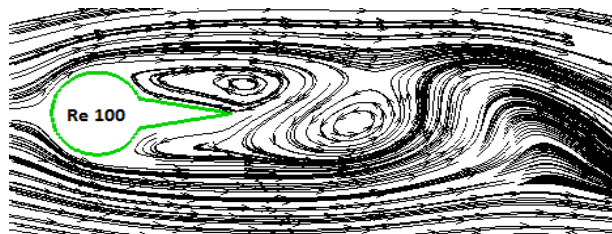


Fig. 6 (c)

Fig. 6 Stream traces of cylinder with triangular wake splitter

C. Effect on wake length

Wake length ( $L_w$ ) in the present work is defined as distance between two stagnation point in the downstream of the cylinder as illustrated in Fig.7. Splitter plates are used as passive means of controlling vortex formation and vortex shedding in the wake. It has been observed that with increase in Reynolds number, the length of wake increases for steady symmetric flow for the entire above mentioned configuration.

Fig. 8 describes variation of wake length with increasing in Reynolds number for steady symmetric flow for bare cylinder, cylinder with rectangular and triangular wake splitters. It is found that wake length for bare cylinder for all the cases of Reynolds number to be more when compared with triangular wake splitter & rectangular wake splitter. It is observed that the wake length for rectangular wake splitter was reduced by 33% and that of triangular wake splitter by 22% when compared to bare cylinder.

D. Pressure and Vorticity contour

Fig.9 describes pressure contours of flow past cylinder with and without wake splitters. For low Reynolds number ( $Re \leq 40$ ), the pressure contours were appeared to be contracted for the wake splitters when compared with the bare cylinder. On the other hand the contours were asymmetric in the downstream and the pressure bubble circulation was observed for wake splitters as compared to a large recirculation region of bare cylinder

The computed vorticity contour is shown in Fig.10 for Reynolds number  $Re=20$  and  $Re=40$  for cylinder with and without wake splitter. The vorticity contours show the high vorticity regions near the wall where the vorticity is generated which consequently diffuses in the downstream due to the fluid viscosity. The close spacing of the vorticity contours in the front half of the cylinder indicates the region of strong transverse velocity gradients in the wall boundary layer. It is also noted, with an increase in Reynolds number vorticity region was found to be increasing in the case of cylinder without wake splitter and cylinder with triangular wake splitter as shown in Fig.10. However the vorticity region for rectangular wake splitter reduced with an increase in the Reynolds number.

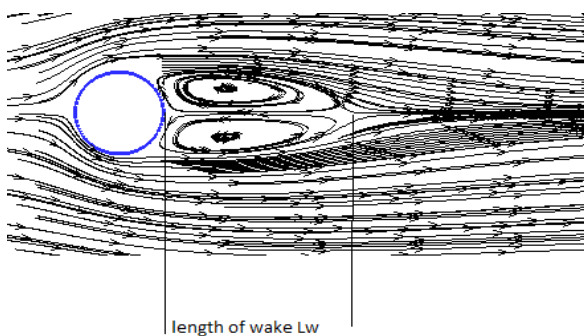


Fig. 7 Length of Wake

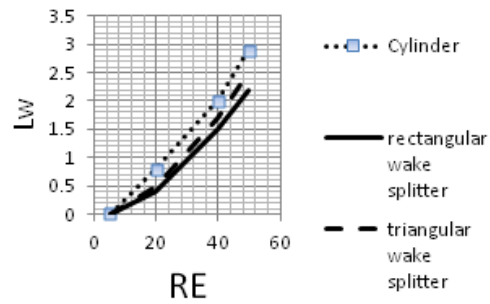


Fig.8 Variation of wake length( $L_w$ ) with Reynolds number( $RE$ ) for steady symmetric flow

Pressure Contours

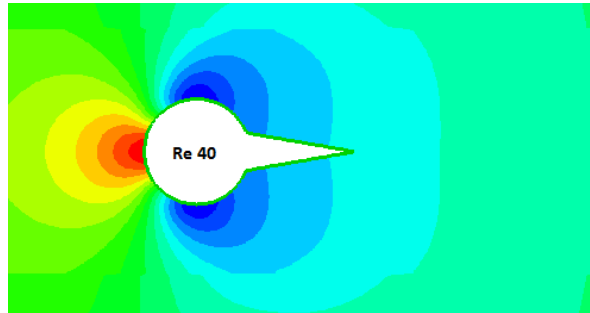


Fig. 9 (a)

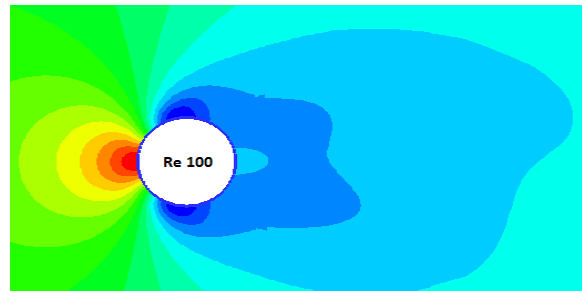


Fig. 9 (b)

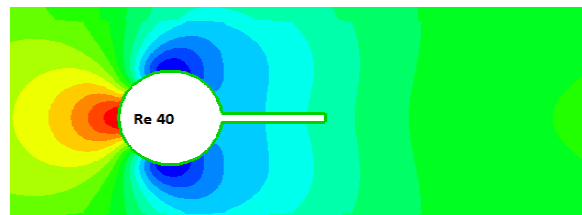


Fig. 9 (c)

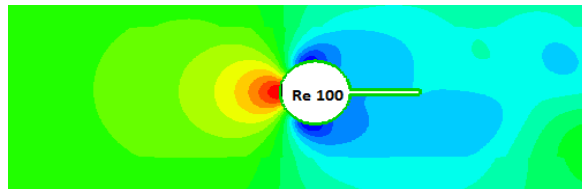


Fig. 9 (d)

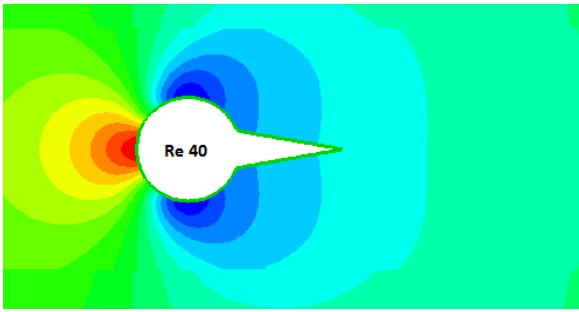


Fig. 9 (e)

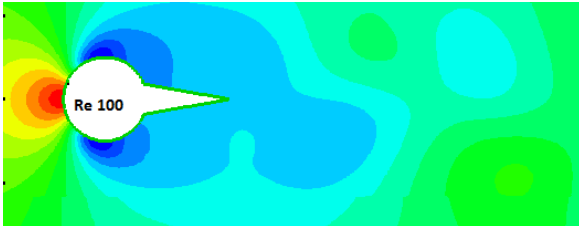


Fig.9 (f)

Fig. 9 Pressure contours

Vorticity Contours

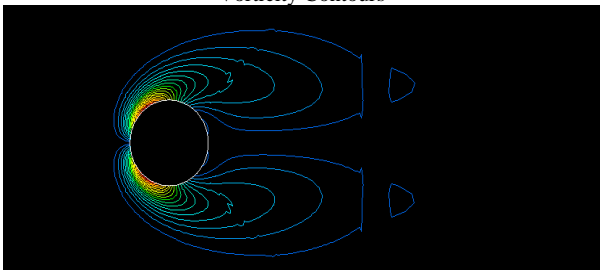


Fig. 10 (a) Re 20

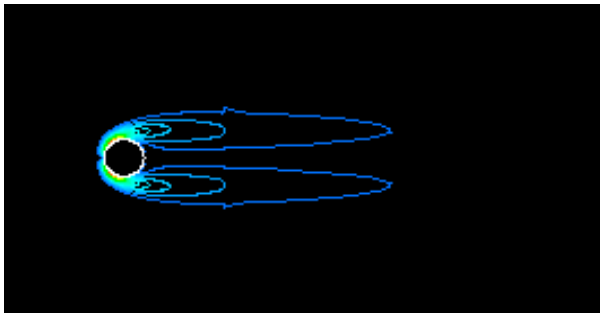


Fig. 10 (b) Re 40

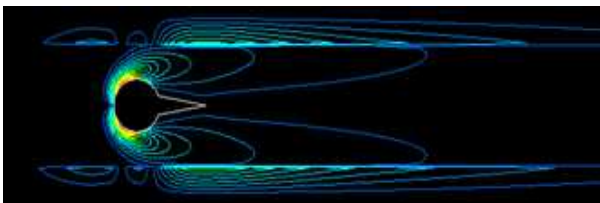


Fig. 10 (c) Re 20

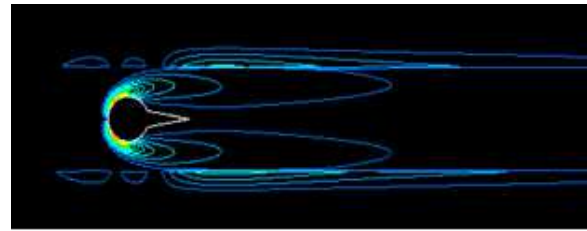


Fig. 10 (d) Re40

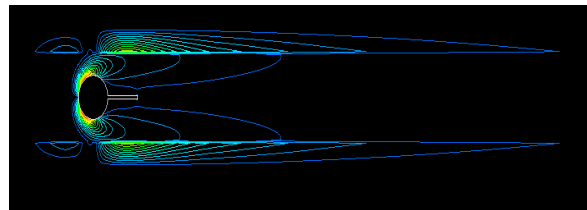


Fig. 10 (e) Re 20

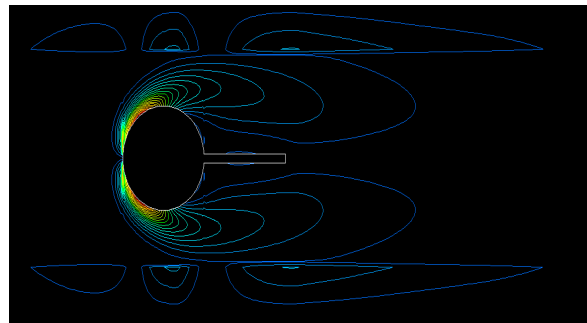
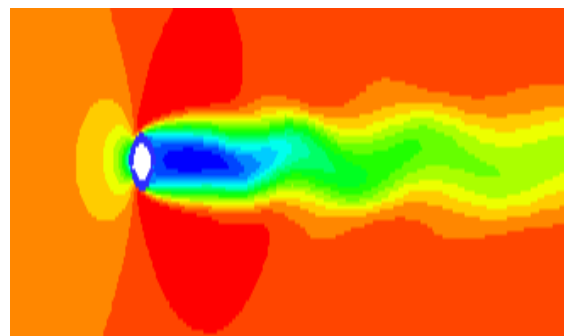


Fig. 10 (f) Re 40

Fig. 10 Vorticity contours

*E. Vortex shedding regime*

The study show that beyond a critical Reynolds number of about 48, the steady closed near wake becomes unstable and a transverse oscillation starts near the end of the wake. As the Reynolds number is increased further, the vortices are shed alternately from the upper and lower cylinder surface at a definite frequency depending on the Reynolds number, leading to Von Karman vortices. Vortex shedding was observed at critical Reynolds number Re 50 in case of cylinder with and without wake splitter.



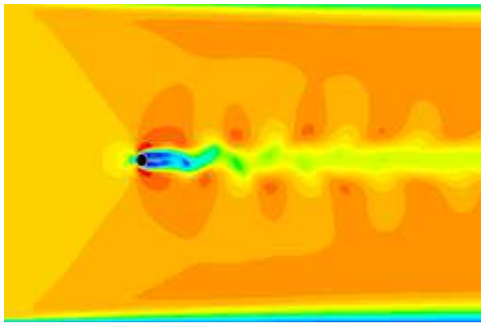


Fig. 11 (b) Rectangular Splitter

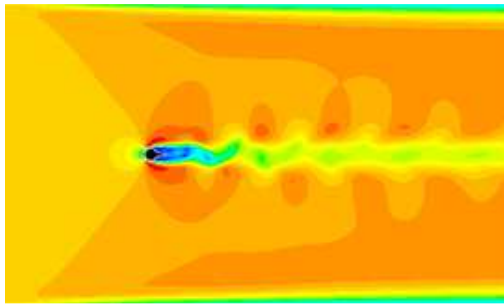


Fig. 11 (c) Triangular Splitter

Fig.11 Von karman vortices at Re 100 for the cylinder with and without wake splitter arrangements

*F. Surface pressure coefficient*

Fig. 12 shows the distribution of pressure coefficient with circumferential distance along the cylinder.

$$C_p = \frac{P - P_\infty}{P_s - P_\infty} \quad (4)$$

P is the local pressure, Ps is the stagnation pressure and  $P_\infty$  is the atmospheric pressure for the case of bare cylinder and cylinder with triangular, rectangular wake splitter. The onset of flow separation on the cylinder surface is usually marked by a notable change in the pressure distribution following separation. The adverse pressure gradient beyond  $\theta=90^\circ$  leads to flow separation. The profile indicates that the pressure in the separated region adjacent to the circular tube is sensitive to wake splitter geometry.

The reason for increase in base pressure due to presence of wake splitter appears to be as follows.

The splitter plates delays the flow separation slightly compared to bare cylinder. The small rise in base pressure is expected to decrease mean drag.

It is predicted from the  $C_p$  graph as mentioned in Fig.12 base pressure for tapered wake splitter is found slightly higher than bare cylinder & cylinder with rectangular wakesplitter.

Mean drag coefficient can be written as

$$C_D = F / 0.5\rho U^2 \infty D \quad (5)$$

where F is mean drag force.

Key note is Mean drag was found lesser on the cylinder with triangular wake splitter. Use of triangular wake splitter was found to be much more effective at Reynolds number 5 as mean Cd was found reduced by 61.36% when compared to rectangular wake splitter and by 65.54% compared to bare cylinder. Comparison of results pertaining to Coefficient of drag for various Reynolds number with and without wake splitters is mentioned in Table II.

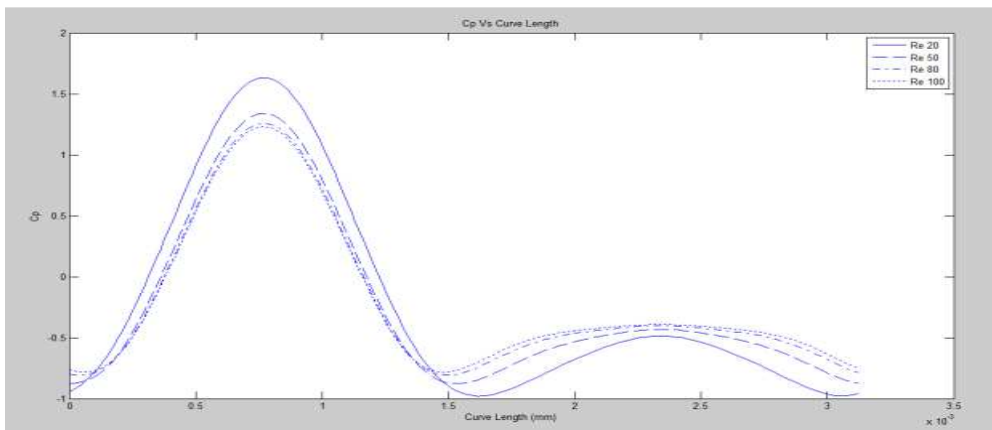


Fig. 12 (a) Bare Cylinder

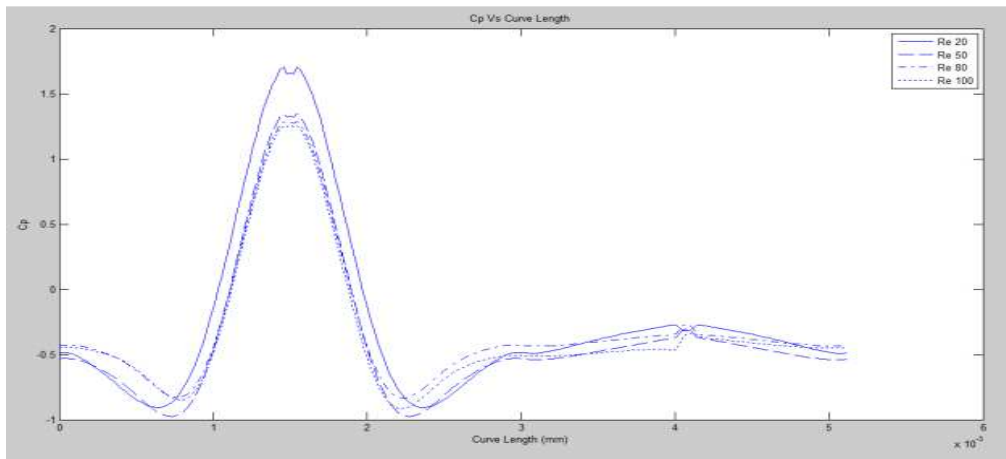


Fig. 12 (b) rectangular splitter

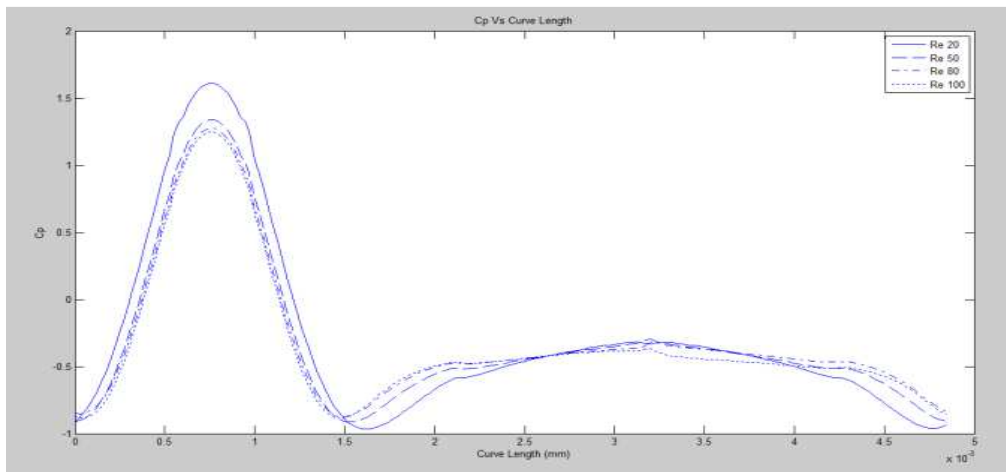


Fig. 12 (c) Triangular splitter

Fig. 12 Cpvs Curve length for bare, rectangular and triangular splitters with variation in Re

TABLE III  
COMPARISON OF MEAN DRAG OF CYLINDER WITHOUT WAKE SPLITTER, CYLINDER WITH RECTANGULAR SPLITTER AND TRIANGULAR SPLITTER

Reynolds No.	Cylinder	Rectangular wake splitter	Triangular Wake Splitter
5	5.92	5.28	2.04
20	2.354	2.358	2.351
40	1.706	1.83	1.687
50	1.55	1.575	1.535
80	1.46	1.284	1.278
100	1.45	1.245	1.237

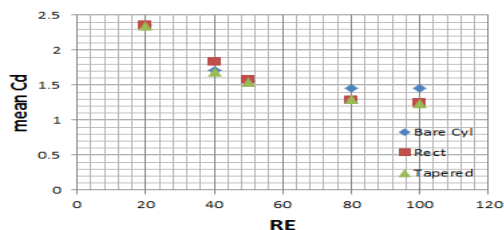


Fig. 13 Coefficient of drag vs Reynolds number

## VI. CONCLUSION

Particular attention has been paid to the study of the variation of coefficient of pressure, mean drag coefficient, stream traces, length of wake with rectangular and taper wake splitter. This study shows increase in the base pressure of triangular wake splitter. Hence reduces the drag on the cylinder which behaves as bluff body thereby improving the aerodynamics of the cylinder. Flow visualization indicates length of wake can be reduced with the use of splitter plates by stabilising the wake formation. The vortices are pushed downstream, followed by narrowing of the wake.

Hence cylinder with triangular wake splitter reduces the mean drag coefficient compared to rectangular wake splitter and bare cylinder. Reduction of drag would be an important aspect on flow over cylinder which can be used to analyse the heat transfer through cylinder.

## REFERENCES

- [1] B.S,V,P.Patnaik ,K.N.Seetharamu,P.AaswathaNarayana simulation of laminar confined flow past a circular cylinder with integral wake splitter

- involving heat transfer. *Int. J. Numer. Method Heat flow Fluid Flow* 6 (1996)
- [2] S.C.R. Dennis, G. Chang, Numerical solutions for steady flow past a circular cylinder at Reynolds numbers up to 100, *J. Fluid Mech.* 42 (1970) 471.
- [3] D. Sucker, H. Brauer, *Fluiddynamik bei der angestromten Zylinder*, *Wärme- und Stoffübertragung* 8 (1975) 149.
- [4] V. Saravanan<sup>1</sup>, C.K. Umesh<sup>1</sup>, B.K. Muralidhara<sup>1</sup>, K.N. Seetharamu<sup>2</sup> national conference on approaching scholastic horizon in mechanics April 2010
- [5] A.L.F. Lima, E. Silva, A. Silveira-Neto, J.J.R. Damasceno Numerical simulation of two-dimensional flows over a circular cylinder using the immersed boundary method. *Int. Computational physics* 189 (2003) 351–370.
- [6] D. Goldstein, R. Hadler, L. Sirovich, Direct numerical simulation of turbulent flow over a modelled riblet covered surface, *J. Comp. Phys.* 302 (1995) 333.
- [7] S. Tiwari, D. Chakraborty, G. Biswas, P. K. Panigrahy, Numerical prediction of flow and heat transfer in a channel in presence of a built-in circular tube with and without wake splitter international journal of heat and mass transfer 48(2005) 439-453
- [8] M.C. Lai, C.S. Peskin, An immersed boundary method with formal second-order accuracy and reduced numerical viscosity, *J. Comp. Phys.* 160 (2000) 705.
- [9] Panchal, Lakdawala, "Numerical investigation of thermal performance in cross flow around square array of circular cylinder" NUI-CONE-2011